



Sub-zero milling of Ti-6Al-4V—impact of the cutting parameters on the resulting forces, tool wear, and surface quality

Kevin Gutzeit¹ · Georgis Bulun² · Gerhard Stelzer² · Benjamin Kirsch¹ · Jörg Seewig² · Jan C. Aurich¹

Received: 5 January 2023 / Accepted: 25 March 2023 / Published online: 31 March 2023
© The Author(s) 2023

Abstract

Due to an excellent ratio of high strength and low density, Ti-6Al-4V is suitable for many industrial applications, especially in the aerospace industry. However, Ti-6Al-4V is also characterized by a very low thermal conductivity and high chemical reactivity which is why the titanium alloy is considered to be a hard-to-cut material. Machining Ti-6Al-4V leads to high cutting temperatures, which leads to a rapidly progressing thermo-chemical induced tool wear. To reduce the thermal load and to enhance the cutting performance, suitable cooling strategies are a necessity. A novel, highly efficient cooling approach is to apply sub-zero metalworking fluids (MWF) at liquid state but at supply temperatures well below 0 °C. These sub-zero MWF inhibit high cooling effects due to their low supply temperature in superposition with a beneficial wetting behavior. In this work, the application of a sub-zero cooling strategy is investigated when milling Ti-6Al-4V. The influence of both down milling and up milling is investigated under a systematic variation of the cutting speed and feed per tooth. For comparison, the experiments are also conducted using a cryogenic CO₂ cooling. The performance of both cooling strategies in dependence of the milling process is described on the basis of the occurring forces, the resulting tool wear, and the surface quality achieved. The results show that the sub-zero cooling can successfully improve the machinability of Ti-6Al-4V even at elevated cutting parameters and unfavorable cutting conditions. As a result, sub-zero milling clearly outperforms the cryogenic CO₂ cooling, since less tool wear and an overall lower surface roughness are observed. Consequently, when using a sub-zero cooling strategy, higher metal removal rates, longer tool life, and better surface qualities are achievable.

Keywords Milling · Sub-zero MWF · Cryogenic · Ti-6Al-4V · Cutting parameters · Roughness

1 Introduction

The titanium alloy Ti-6Al-4V is characterized by an excellent ratio of high strength even at elevated temperatures to a low density [1, 2]. This beneficial characteristic leads to a high suitability for industrial applications, especially in the aerospace industry [3, 4]. In addition, the titanium alloy exhibits a high corrosion resistance and favorable biological properties, which is why Ti-6Al-4V is also widely used for offshore [5], chemical [6], and medical [7, 8] applications.

However, Ti-6Al-4V inhibits a very low thermal conductivity in addition to a low heat capacity which causes difficulties in heat dissipation when cutting [9]. As a consequence, the heat dissipation via the workpiece and chips is limited [10, 11] which leads to high cutting temperatures and thus high thermal loads at the cutting edge [12]. Additionally, Ti-6Al-4V is also characterized by a very high chemical reactivity, especially at elevated temperatures. When cutting, this reactivity leads to adhesive and chemical reactions between the titanium alloy and the tool [13, 14]. These reactions in superposition with the high thermal loads result in rapidly progressing tool wear which reduces tool life and thus the productivity of the cutting process [15]. In conclusion, Ti-6Al-4V is regarded as a hard-to-cut material [16].

To reduce the thermal load and consequently the thermo-chemical induced tool wear when cutting Ti-6Al-4V, a very low cutting speed is generally chosen [17]. This however results in low productivity which is why machining Ti-6Al-4V is often associated with high manufacturing

✉ Kevin Gutzeit
kevin.gutzeit@mv.uni-kl.de

¹ Institute for Manufacturing Technology and Production Systems, RPTU Kaiserslautern, Gottlieb-Daimler-Str, 67663 Kaiserslautern, Germany

² Institute for Measurement and Sensor Technology, RPTU Kaiserslautern, Gottlieb-Daimler-Str, 67663 Kaiserslautern, Germany

costs [18]. Lower cutting speeds also tend to increase the occurring forces when milling, as no thermal softening takes place [19]. In addition, up milling has to be generally avoided, since the process kinematic promotes higher thermo-mechanical loads in comparison to down milling due to ploughing effects [20]. Other attempts to improve the machinability of the titanium alloy rely on the use of coatings [21] or cutting edge preparation [22, 23]. While a defined cutting edge rounding offers the potential to increase tool life due to a higher mechanical strength of the cutting edge, the increased cutting edge radius also promotes ploughing effects and therefore more friction and higher thermo-mechanical loads [22, 24].

Another, more efficient, approach to reduce the thermal load and improve the machinability of Ti-6Al-4V is the application of cryogenic cooling strategies, typically with liquid nitrogen (LN₂) or carbon dioxide snow (CO₂) [25]. During cryogenic milling, the high cooling effect is achieved due to the extremely low supply temperatures of LN₂ (−196 °C [26]) or CO₂ (−78.5 °C [27]) promoting a high temperature gradient [28]. Additionally, cryogenic cooling strategies are often regarded as an environmentally friendly and sustainable alternative in comparison to the application of conventional metalworking fluids (MWF) [29].

In recent years, a lot of research has been conducted regarding the application of cryogenic cooling strategies for milling Ti-6Al-4V. For example, Sadik et al. [30] were able to increase tool life during face milling Ti-6Al-4V when using a cryogenic CO₂ cooling instead of a conventional MWF. Investigations of Pittalà [31] showed that increasing the CO₂ mass flow could reduce tool wear, since lower temperatures and better cooling performance are achieved. When cryogenic milling Ti-6Al-4V, Iqbal et al. [32] observed a better machinability when changing from up milling to down milling. This is attributed to the favorable process kinematic resulting in less friction and ploughing. By combining an internal cryogenic cooling with a minimum quantity lubrication (MQL), Park et al. [33] were able to further improve tool life while end milling Ti-6Al-4V.

However, it has also been shown that the cryogenic milling has its limits when machining Ti-6Al-4V. Wika et al. [34] could demonstrate that no significant improvement of the tool life is obtained at elevated cutting parameters ($v_c = 80$ m/min) even when combining the cryogenic cooling with an MQL. The same observation was made by Tapoglou et al. [35] when using a cutting speed of $v_c = 100$ m/min. In both cases, the cryogenic coolant was outperformed by a conventional flood cooling. The authors concluded that the lack of lubrication when using a cryogenic cooling has a decisive negative impact on the cutting performance. This is especially evident at higher cutting speeds, since the amount of friction and heat being generated is increased drastically [34, 35]. In comparison to a

cryogenic cooling, a conventional MWF supplied at liquid state inhibits much better lubrication effects and additionally a promoted wetting behavior. However, their supply temperature is generally limited to temperatures above 0 °C, hampering their cooling performance [28, 36]. The results provided by literature show that the performance of the applied cooling strategy is strongly impacted by the applied milling strategies and the resulting occurring loads. To improve the machinability of Ti-6Al-4V, especially at elevated cutting speeds, a suitable cooling strategy should provide high cooling capacities and beneficial lubrication properties.

Mixtures of water and polyhydric alcohols, so-called sub-zero MWF, offer the potential to combine the benefits from cryogenic and conventional flood cooling [37]. These sub-zero MWF can be applied at supply temperatures well below 0 °C while maintaining their liquid state. This enables high cooling effects due to the combination of low supply temperatures and a beneficial wetting behavior [37, 38]. The promoted heat transfer in superposition with the lubrication effects of the sub-zero MWF promotes a lower thermo-mechanical load when machining Ti-6Al-4V [39]. In previous works, the application of sub-zero cooling strategies resulted in less tool wear [40] and an optimized surface integrity [41, 42] when turning Ti-6Al-4V. While milling Ti-6Al-4V, a favorable thermo-mechanical load has also been observed by us, which resulted in a better surface quality compared to a cryogenic cooling strategy [43].

By now, the application of sub-zero MWF for milling operations is very limited and has so far only been investigated at comparably low cutting speeds ($v_c = 50$ m/min) [43]. However, the cutting parameters chosen have a decisive impact on the performance of the cooling strategy and the respective cutting process. Therefore, the aim of this paper is to characterize the performance of a sub-zero cooling strategy in dependence of the cutting parameters during milling and the respective occurring loads. For reference, the performance of the sub-zero cooling strategy will be compared with a cryogenic CO₂ cooling. In addition, the impact of up milling vs. down milling will also be investigated. The influence of the respective cooling and milling strategies on the milling process will be characterized by the occurring forces, as they are suitable to indicate the process stability as well as the overall machinability when milling Ti-6Al-4V [19, 44]. In addition, the resulting tool wear and the surface quality achieved are analyzed and compared. As an outcome of this paper, the results presented allow a comprehensive evaluation regarding the performance of a highly efficient sub-zero cooling strategy for a broad variety of milling operations. This in term offers high potential to improve the overall machinability of the hard-to-cut titanium alloy Ti-6Al-4V.

2 Experimental setup

2.1 Machining experiments

Solution annealed Ti-6Al-4V workpieces with a cross section of $A = 10 \times 10 \text{ mm}^2$ and a length of $l = 100 \text{ mm}$ were machined via end milling. The milling experiments were all carried out on a 5-axis machining center (Deckel Maho Gildemeister DMU 70 eVolution¹). The experimental setup is depicted in Fig. 1.

The combination of two cooling strategies and two milling strategies was investigated resulting in the four cases listed in Table 1. For each case, the influence of the cutting parameters was investigated by systematically varying the cutting speed and the feed per tooth (see Table 1). Consequently, a total of 36 different setups were investigated.

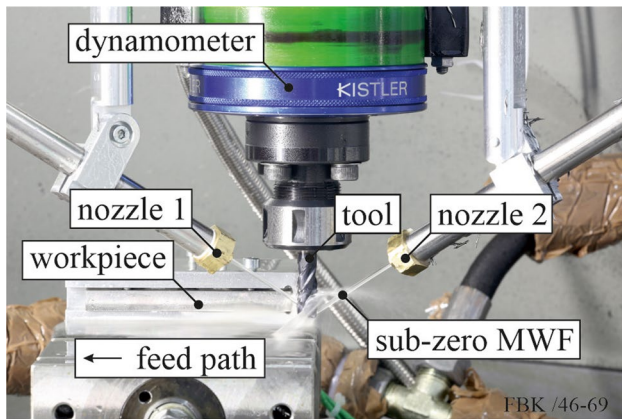


Fig. 1 Depiction of the experimental setup when using the sub-zero MWF

For statistical verification, three tests were conducted with the same end mill for each setup. To characterize the influence of the cooling and milling strategy on the resulting tool wear, a new end mill was used for every setup investigated. The tools used are further specified in Table 2. Before starting each test, a uniform workpiece temperature of $20 \text{ }^\circ\text{C}$ was ensured using type K thermocouples (NiCr-Ni).

For the sub-zero MWF, a mixture of water and ethane-1,2-diol (MEG) was used. The mass ratio of that mixture was $\zeta_{\text{MEG,Water}} = 1.72 \text{ g/g}$ of MEG and water, which corresponds to a composition of 0.33 mol MEG per 1 mol of sub-zero MWF. An alkyl phosphate was added as an anti-wear agent ($\text{C}_{12}\text{H}_{27}\text{O}_4\text{P}$) with a concentration of 14 g per 1 kg of sub-zero MWF. Additionally, 3.7 g of disodium metasilicate (Na_2SiO_3) was added per 1 kg of sub-zero MWF as a corrosion inhibitor. The supply temperature of the sub-zero MWF was set to $T_{\text{sub-zero}} = -30 \text{ }^\circ\text{C}$. The sub-zero MWF was supplied to the cutting zone via two nozzles with a respective outlet diameter of $d = 1 \text{ mm}$ at a constant volume flow of $\dot{V} = 2.7 \text{ L/min}$. The temperature and the volume flow were measured using a Coriolis flow meter (Siemens FCS 400¹).

Table 2 Specification of the milling tool used (manufacturer’s information)

Tool: RF 100 Ti (Gühring KG ¹)	
DK 460 UF	WC: 90%, Co 10%
Coating	Ti–Al–N
Diameter	$D = 10 \text{ mm}$
Number of teeth	$z = 4$
Cutting edge radius	$r_\beta = 5 \text{ }\mu\text{m}$
Corner radius	$R = 0.5 \text{ mm}$
Helix angle	$\beta_1 = 35^\circ; \beta_2 = 38^\circ$

Table 1 Cases and process parameters investigated

Case	Cooling strategy	Milling strategy
1	Sub-zero	Down milling
2	Sub-zero	Up milling
3	CO_2	Down milling
4	CO_2	Up milling
v_c in m/min	f_z in mm	a_e in mm
50	0.04	1
100	0.04	1
150	0.04	1
50	0.08	1
100	0.08	1
150	0.08	1
50	0.12	1
100	0.12	1
150	0.12	1
		a_p in mm
		10
		10
		10
		10
		10
		10
		10
		10

For the experiments with CO₂ cooling, the cryogenic coolant was stored at ambient temperature in a siphoned gas cylinder. With an outlet temperature of $T_{\text{CO}_2} = -78.5\text{ }^\circ\text{C}$ [27] and a mass flow of $\dot{m} = 0.7\text{ kg/min}$, the CO₂ was supplied to the cutting zone via two nozzles. Each nozzle had an outlet diameter of $d = 0.5\text{ mm}$. The mass flow was estimated by measuring the weight loss of the gas cylinder with a weighting platform. Both supply techniques were adapted from previous investigations [45], as they provide favorable cooling capacities.

2.2 Measurement technology

Using a rotating dynamometer (Kistler Type 9123C¹), the three force components F_x , F_y , and F_z were measured at the tool during milling. A sampling frequency of 15 kHz was used. The force measurements were triggered using the NC code of the machining center to ensure a uniform start and end of the respective measurement. In Fig. 2, the orientation of the three force components is schematically depicted.

A representative measurement of each force component over the feed path is given in Fig. 3. Due to the rotation of the tool, the force components F_x and F_y acting on the tool show similar characteristics. However, the forces measured regarding F_y seem to be slightly higher, which can be attributed to the different helix angles of the tool (see Table 2). Increasing the helix angle influences the ratio between axial and radial force components as well as the geometry of the flute. This in turn highly impacts the chip formation, the process stability regarding vibrations, and consequently the occurring forces. When milling Ti-6Al-4V, this influence of the helix angle on the occurring forces has also been observed by Iqbal et al. [32].

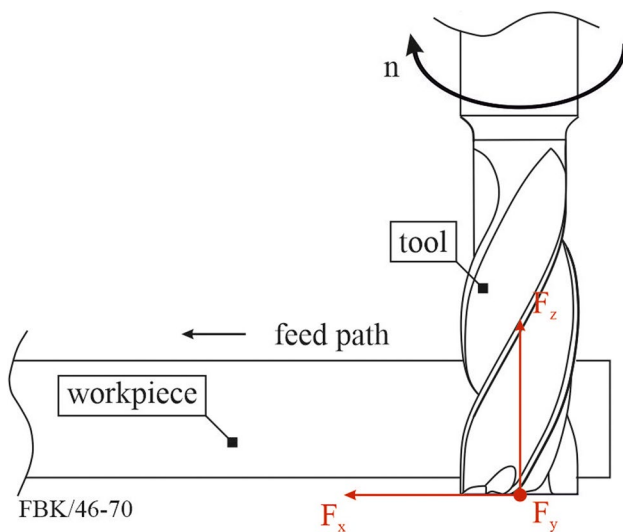
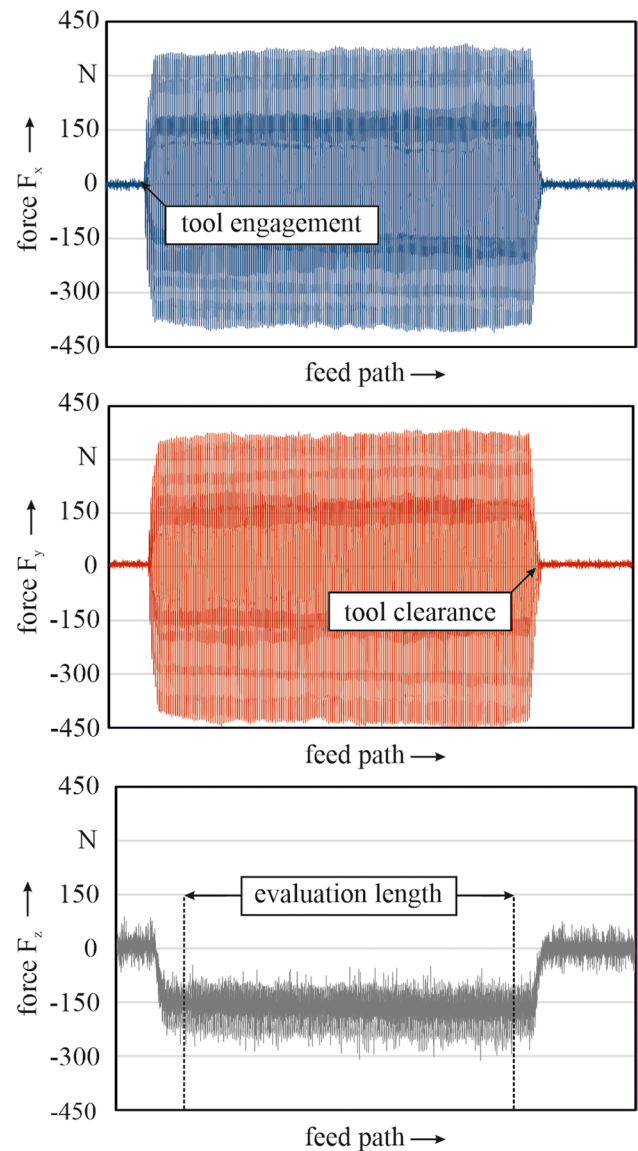


Fig. 2 Schematic depiction of the orientation of the force components



workpiece:	tool: RF 100 Ti
Ti-6Al-4V	cemented carbide: DK 460 UF, $z = 4$
$10 \times 10 \times 100\text{ mm}^3$	coating: Ti-Al-N, $D = 10\text{ mm}$, $r_\beta = 5\text{ }\mu\text{m}$
cutting parameters:	cooling strategy: sub-zero
$a_e = 1\text{ mm}$, $v_c = 150\text{ m/min}$	$T_{\text{Sub-zero}} = -30\text{ }^\circ\text{C}$
$a_p = 10\text{ mm}$, $f_z = 0.08\text{ mm}$	$\dot{V} = 2.7\text{ l/min}$
	FBK/46-71

Fig. 3 Representative measurement signal of the forces occurring on the tool during milling

The entrance and exit of the tool are clearly visible for each force component. In order to prevent possible errors resulting from the tool engagement and tool clearance, a uniform evaluation length over the feed path was maintained. Within this evaluation length, the RMS was calculated for each force component to determine the resulting force F_{Res} via Eq. 1.

$$F_{\text{Res}} = \sqrt{F_x^2 + F_y^2 + F_z^2} \quad (1)$$

Tool wear was characterized using an optical microscope (Olympus SZ61¹). The state of the tool was observed after all three tests of the respective setup were conducted. This corresponds to a cumulated milling path of $l_f = 300$ mm.

The influence of the cryogenic and sub-zero milling process on the surface quality was determined via optical measurements of the surface topography. A confocal microscope (NanoFocus AG, $\mu\text{surf expert}^1$) was used with an objective with a $20\times$ magnification and a numerical aperture of 0.6 with a lateral resolution of $0.67 \mu\text{m} \times 0.67 \mu\text{m}$. All samples were cleaned and clamped in a sample holder to assure that a similar location is measured during all measurements. For some samples that were milled via up milling, chips and adhesions were welded onto the surface. In order to conduct a proper optical measurement, these artifacts had to be removed carefully during the cleaning process (see

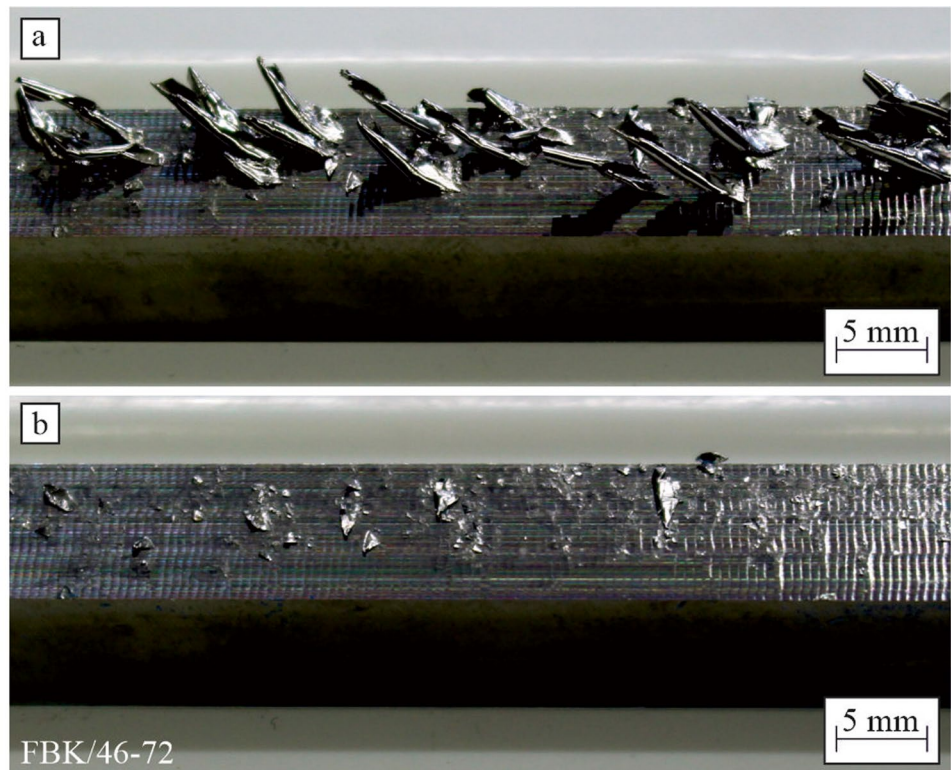
Fig. 4). The measurements were evaluated to determine the root mean square height Sq according to ISO 25178 [46].

3 Results and discussion

3.1 Impact on the occurring process forces during cryogenic and sub-zero milling

In Fig. 5, the resulting forces occurring when down milling are depicted in dependence of the cutting parameters for cryogenic (a) and sub-zero milling (b). Increasing the feed per tooth leads to higher resulting forces independent of the cooling strategy or the cutting speed. Because of the higher undeformed chip-cross section at a higher feed per tooth, more material has to be removed per cut. This results in higher forces which is also observed for dry milling [19] and conventional flood cooling when milling Ti-6Al-4V [47].

Fig. 4 Representative depiction of a surface generated via up milling before (a) and after (b) the removal of adhered chips



workpiece:

Ti-6Al-4V

$10 \times 10 \times 100 \text{ mm}^3$

cutting parameters:

$v_c = 150 \text{ m/min}$; $a_e = 1 \text{ mm}$, external CO_2 -cooling

$f_z = 0.04 \text{ mm}$; $a_p = 10 \text{ mm}$ $T_{\text{CO}_2} = -78.5^\circ\text{C}$, $m = 0.7 \text{ kg/min}$

tool: RF 100 Ti

cemented carbide: DK 460 UF, $z = 4$

coating: Ti-Al-N, $D = 10 \text{ mm}$, $r_\beta = 5 \mu\text{m}$

cooling strategy: cryogen

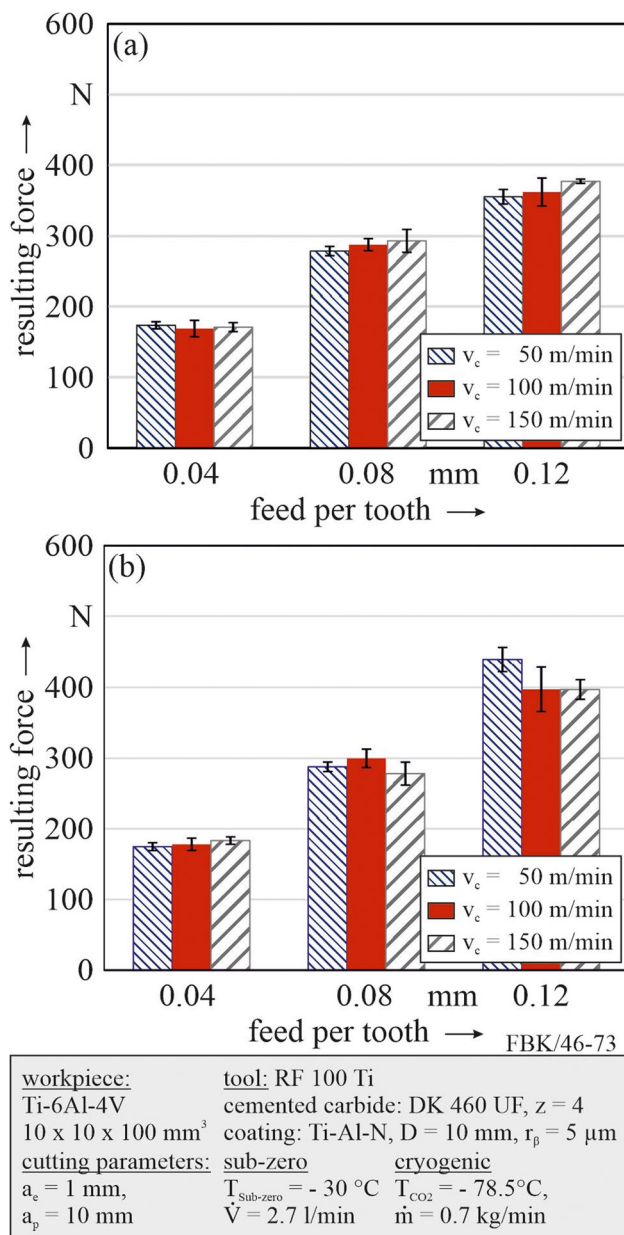


Fig. 5 Resulting forces in dependence of the cutting parameters when down milling using a cryogenic and b sub-zero cooling strategy

Regarding the cutting speed, no significant influence is observed at a constant feed per tooth of $f_z \leq 0.08$ mm for both cooling strategies. However, at an elevated feed per tooth ($f_z = 0.12$ mm) slightly higher resulting forces are observed when increasing the cutting speed during cryogenic milling. In general, decreasing forces are expected when increasing the cutting speed, due to higher thermal loads which induce thermal softening [19, 48]. For cryogenic milling, however, this did not occur here. A possible explanation is the alteration of the cutting edge geometry, due to tool wear in form of adhesions and build-up edges.

When machining Ti-6Al-4V, this is promoted by high thermal loads which are expected especially at increased cutting speeds [49]. The influence of the process parameters during cryogenic milling on tool wear is further discussed in Sect. 3.2.

During sub-zero milling, the resulting forces increase slightly at $v_c = 50$ m/min only when regarding the highest feed per tooth investigated ($f_z = 0.12$ mm). This might be explained by the lack of thermal softening since the lowest thermal loads are expected here. Despite that, the influence of the cutting speed when changing from $v_c = 100$ to $v_c = 150$ m/min is comparably low. Another possible explanation could be the unfavorable ratio between the low cutting speed and a high feed per tooth. This parameter setting could enhance the development of build-up edges, resulting in higher mechanical loads due to a change of the cutting edge geometry.

When comparing cryogenic and sub-zero down milling, the occurring resulting forces are generally within the same magnitude. However, the resulting forces occurring during cryogenic milling are slightly lower, especially at elevated cutting speeds. It is assumed that the lack of beneficial lubrication effects during cryogenic milling leads to more friction and therefore higher thermal loads especially at higher cutting temperatures. While the sub-zero MWF offers better lubrication, therefore reducing the friction, the higher cooling efficiency of the sub-zero cooling also counteracts the thermal softening. Consequently, it seems as if the thermal softening has a higher impact regarding the resulting forces in comparison to the reduction of friction via lubrication for down milling operations.

The resulting forces occurring during up milling are given in Fig. 6 in dependence of the cutting parameters and the cooling strategy applied. Similar to down milling, the resulting forces increase at higher feeds per tooth during up milling for both cooling strategies, due to an increased undeformed chip-cross section.

When changing from cryogenic down milling (Fig. 5a) to cryogenic up milling (Fig. 6a), higher forces are generally observed with the exception of two parameter combinations ($f_z = 0.8$ mm, $v_c = 50$ m/min/ $f_z = 0.08$ mm, $v_c = 100$ m/min). Due to its kinematic, up milling does promote a higher amount of plastic deformation in the workpiece surface layer. This can result in ploughing effects with higher mechanical loads. Increasing forces at higher cutting speeds are clearly observed when an elevated feed per tooth ($f_z \geq 0.08$ mm) was chosen. At a feed per tooth of $f_z = 0.12$ mm, the standard deviation increases at higher cutting speeds. A significant increase of the standard deviation is also observed for the parameter combination of $f_z = 0.08$ mm and $v_c = 150$ m/min. The increased standard deviations do support the hypothesis of a rapidly increasing tool wear, which is later discussed in Sect. 3.2.

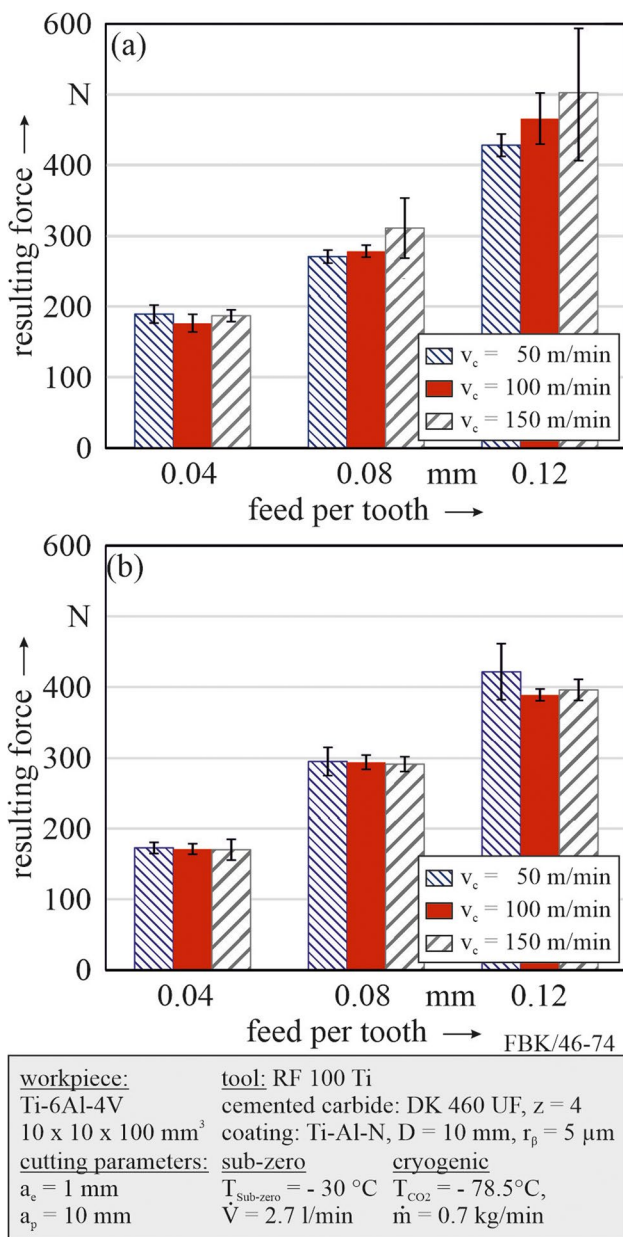


Fig. 6 Resulting forces in dependence of the cutting parameters when up milling using a a cryogenic and b sub-zero cooling strategy

When changing from down milling (Fig. 5b) to up milling (Fig. 6b) while applying the sub-zero MWF, no significant change of the resulting forces occurs for every cutting parameter combination investigated. A possible explanation is given by the favorable lubrication effects of the liquid sub-zero MWF. It is assumed that these lubrication effects reduce the friction when cutting which might counteract the ploughing effects occurring during up milling.

During up milling, generally higher forces are observed for cryogenic milling in comparison to sub-zero milling. This is especially evident for high feeds per tooth and high

cutting speeds. Despite the influence of thermal softening and friction, it is assumed that rapidly progressing tool wear has a decisive impact here. The characterization of the tool wear is discussed in the following chapter.

3.2 Influence of the cutting parameters on the resulting tool wear after cryogenic and sub-zero milling

Depictions of the milling tools used for cryogenic milling and sub-zero milling in dependence of the cutting parameters and the milling strategy are given in Fig. 7 and Fig. 8 respectively. Here, a representative cutting edge of each tool is shown after a cumulated feed path of $l_f = 300$ mm. For down milling (Fig. 7), no significant tool wear is observed for the majority of the investigated parameter settings for both cooling strategies applied. When applying the cryogenic coolant, minor adhesions are observed at the cutting edge at an elevated cutting speed ($v_c = 150$ m/min) and feed per tooth ($f_z = 0.12$ mm). These adhesions result from the chemical reactivity of the titanium alloy which is promoted at elevated temperatures. Since the thermal load increases at higher cutting speeds and feeds per tooth, higher thermal loads occur which is why adhesions are observed here. These adhesions can alter the geometry of the cutting edge, which can explain the slightly increased resulting forces when down milling using this setting of cutting parameters (see. Figure 5a). For sub-zero down milling, no significant amount of adhesions is observed at the cutting edges of the tools, independent of the cutting parameters used.

After cryogenic up milling (Fig. 8), adhesions are observed at the cutting edge of the respective tools for the majority of parameter settings investigated. The amount and/or size of adhesions observed increases with higher feeds per tooth and especially with higher cutting speeds. When comparing the milling strategies while using the cryogenic cooling strategy, up milling leads to a significantly increased tool wear, for most of the cutting parameter settings investigated. This is attributed to the process kinematic during up milling, since ploughing effects are promoted here, which further increase friction and therefore the occurring thermal loads and the resulting adhesions.

For up milling, the progressing tool wear does significantly affect the occurring forces, which is why increased standard deviations and higher resulting forces are observed if an increased tool wear occurs (see. Fig. 6a).

After sub-zero up milling, no significant amount of adhesions is observed at the cutting edges of the tools with the exception of one cutting parameter setting ($v_c = 150$ m/min, $f_z = 0.12$ mm). Here some minor adhesions are visible. Hence, despite the higher thermal loads that are expected at increased cutting parameters and the unfavorable process kinematic during up milling, the sub-zero cooling does

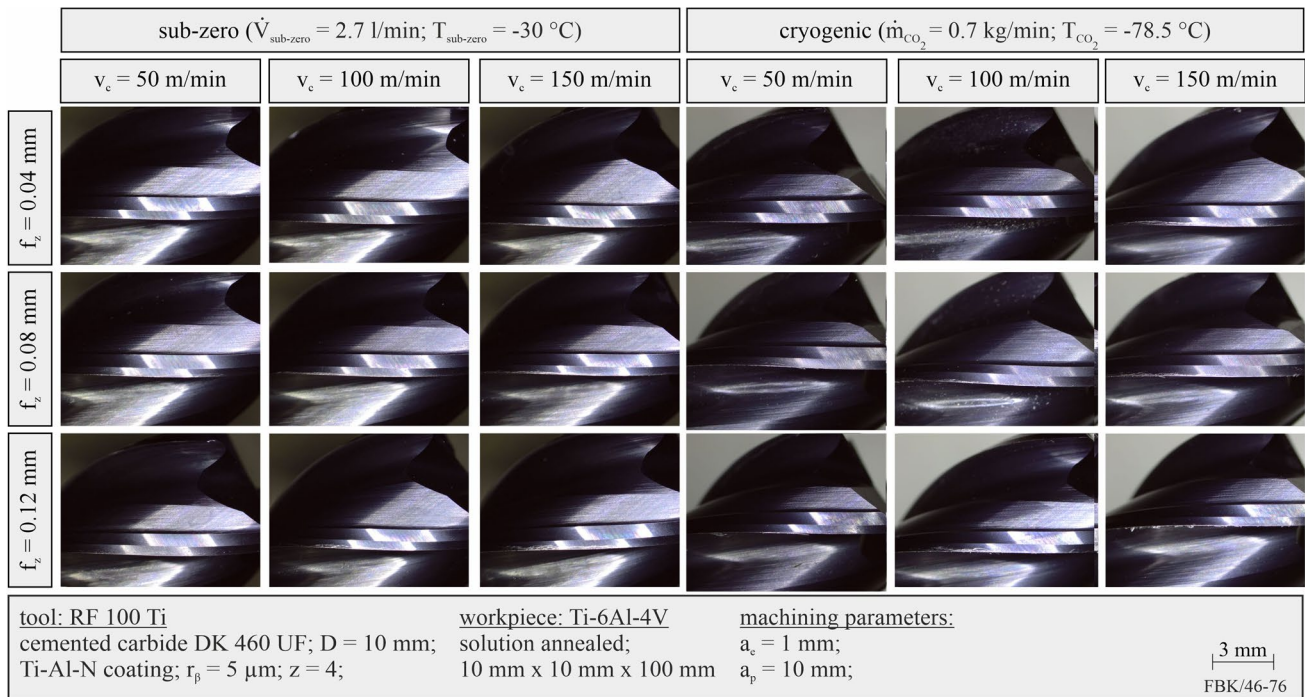


Fig. 7 Depiction of the tool after a feed path of $l_f = 300 \text{ mm}$ in dependence of the cutting parameters and cooling strategy when down milling

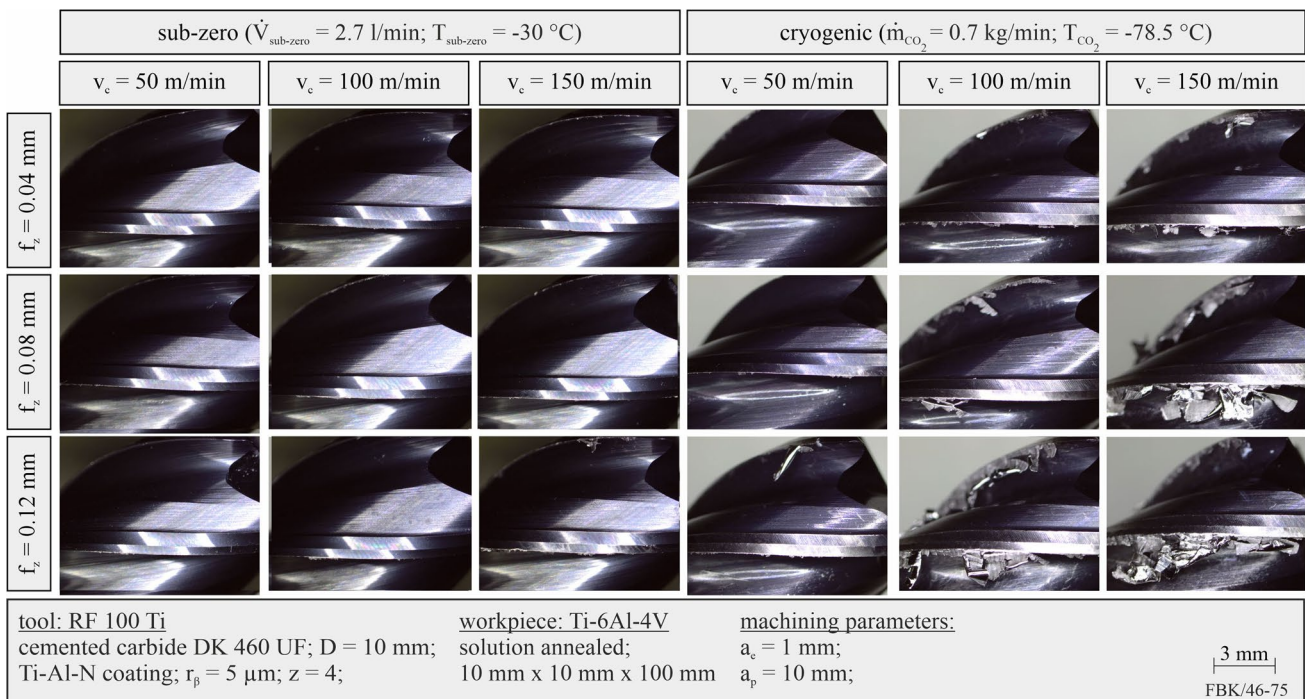


Fig. 8 Depiction of the tool after a feed path of $l_f = 300 \text{ mm}$ in dependence of the cutting parameters and cooling strategy when up milling

effectively reduce the thermal load to counteract the formation of adhesions at the cutting edge.

3.3 Surface quality realized after cryogenic and sub-zero milling

To characterize the influence of the milling process and the cooling strategy on the surface quality, representative depictions of the surface topography at a constant feed per tooth are given in Fig. 9 ($f_z=0.04$ mm), Fig. 10 ($f_z=0.08$ mm), and Fig. 11 ($f_z=0.12$ mm).

When comparing the three figures, the influence of the feed per tooth on the surface topography can be seen. At higher feeds per tooth, the distance and height of the feed marks increase, due to the change of the process kinematic which is in line with the results obtained by Zain et al. [50]

and Karkalos et al. [51]. At a constant feed per tooth, the process kinematic and therefore the kinematic roughness resulting from the milling process are identical for all cases investigated. In addition to the influence of the kinematic roughness on the surface topography, other surface artifacts are also observed in dependence of the milling and cooling strategy. When using a cryogenic cooling during down milling, small amounts of adhesions (e.g., Fig. 9: $v_c=100$ m/min) and scratches (e.g., Fig. 9: $v_c=150$ m/min) are visible at the workpiece surface for some of the cases investigated. It is likely that these scratches result from chips which were dragged across the workpiece surface. The amount of adhesions increases significantly when changing from down milling to up milling, especially at higher feeds per tooth and higher cutting speeds. At the lowest feed per tooth investigated ($f_z=0.04$ mm), these adhesions

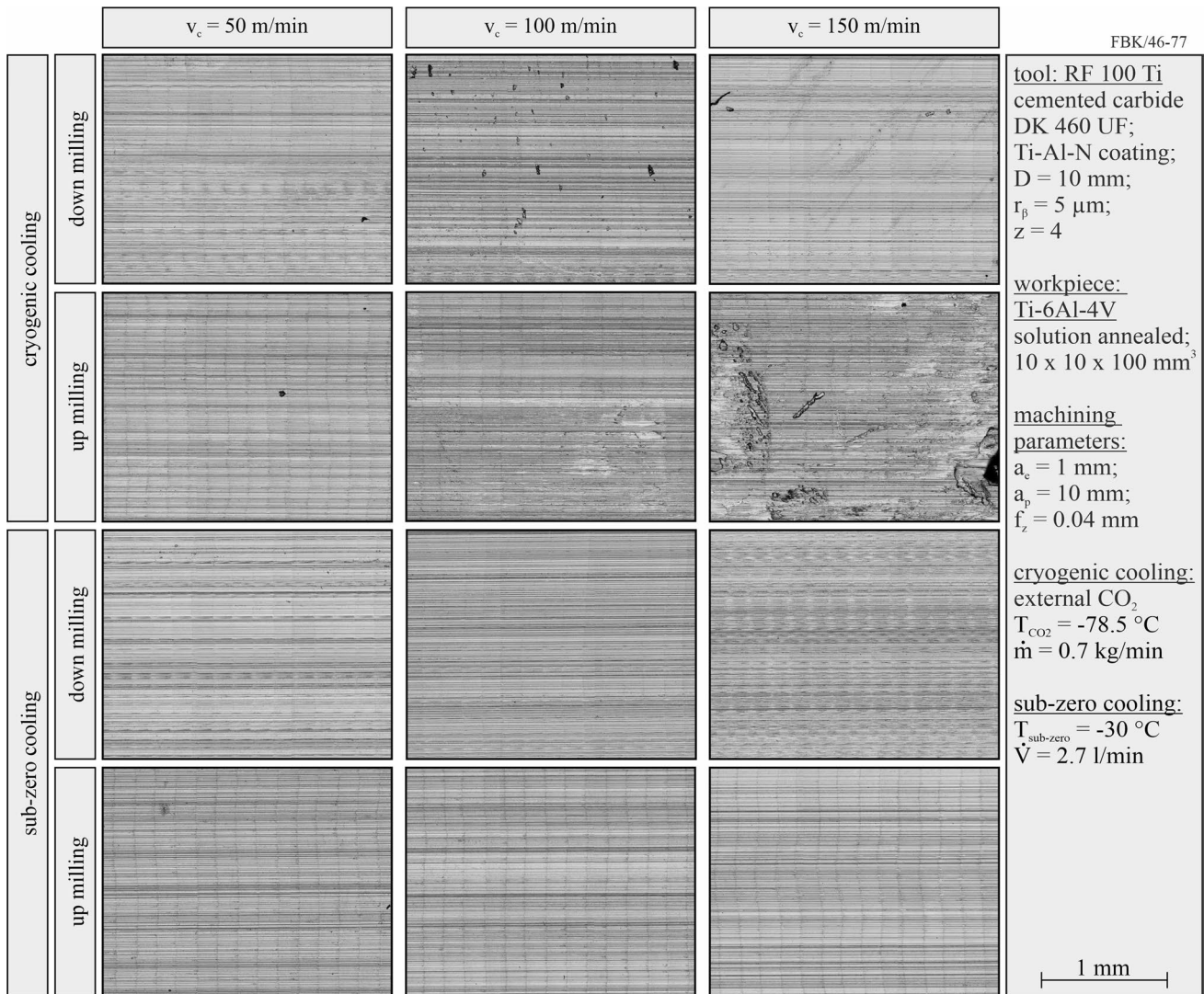


Fig. 9 Representative depiction of the surface topography at a constant feed per tooth of $f_z=0.04$ mm in dependence of the milling and cooling strategies

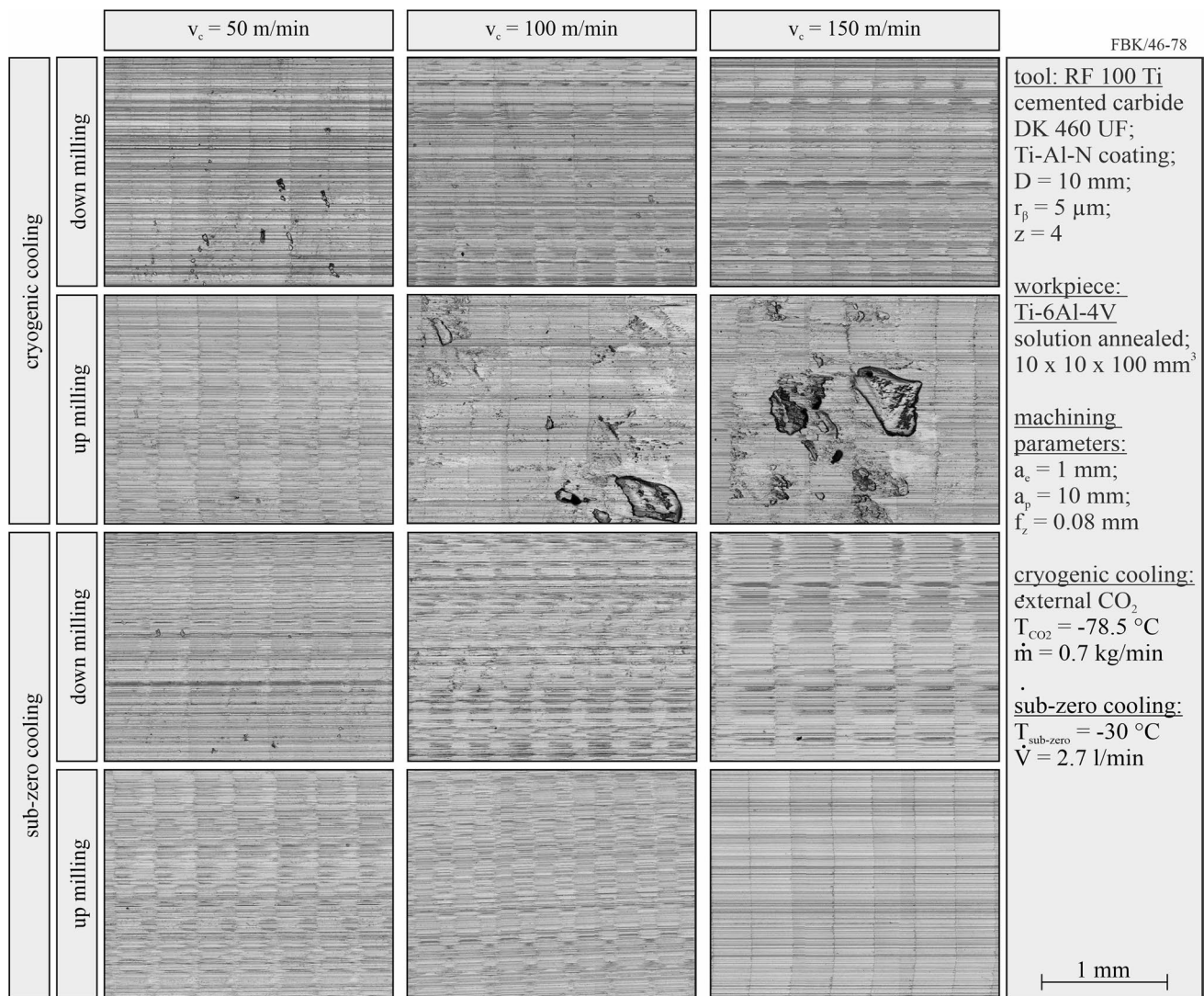


Fig. 10 Representative depiction of the surface topography at a constant feed per tooth of $f_z = 0.08$ mm in dependence of the milling and cooling strategies

are only present when using the highest cutting speed of $v_c = 150$ m/min (see Fig. 9). At the highest feed per tooth of $f_z = 0.12$ mm, adhesions are observed on the workpiece surface for every cutting speed investigated (see Fig. 11). This deterioration of the surface quality due to adhesions results from the high thermal loads within the cutting zone. These loads are enhanced by ploughing effects due to the process kinematic and the elevated cutting parameters which highly increase the friction and therefore the occurring temperature. The occurrence and magnitude of the adhesions that occur during cryogenic up milling are in line with the tool wear that is also observed for these respective cases (see. Figure 7 and Fig. 8). After sub-zero milling, no severe artifacts are observed on the workpiece surface regardless of the milling strategy, or the combination of process parameters used. Even at unfavorable cutting conditions like high cutting

speeds or after up milling, no adhesions did occur on the workpiece surface. This is also in line with the observations made regarding the tool wear (see Fig. 7 and Fig. 8) where no significant alterations of the cutting edges were found after sub-zero milling regardless of the milling strategy and the cutting parameters investigated.

In comparison to the cryogenic CO₂ cooling, the occurrence of artifacts on the workpiece surface is clearly reduced when using the sub-zero cooling for both down milling and up milling and for every combination of cutting parameters investigated. The superior performance of the sub-zero cooling can be explained by the enhanced cooling capacity which effectively decreases the thermal load even at unfavorable cutting conditions (up milling, increased cutting parameters). This sufficient reduction of the thermal loads counteracts the formation of adhesions at the workpiece surface. In addition, the sub-zero

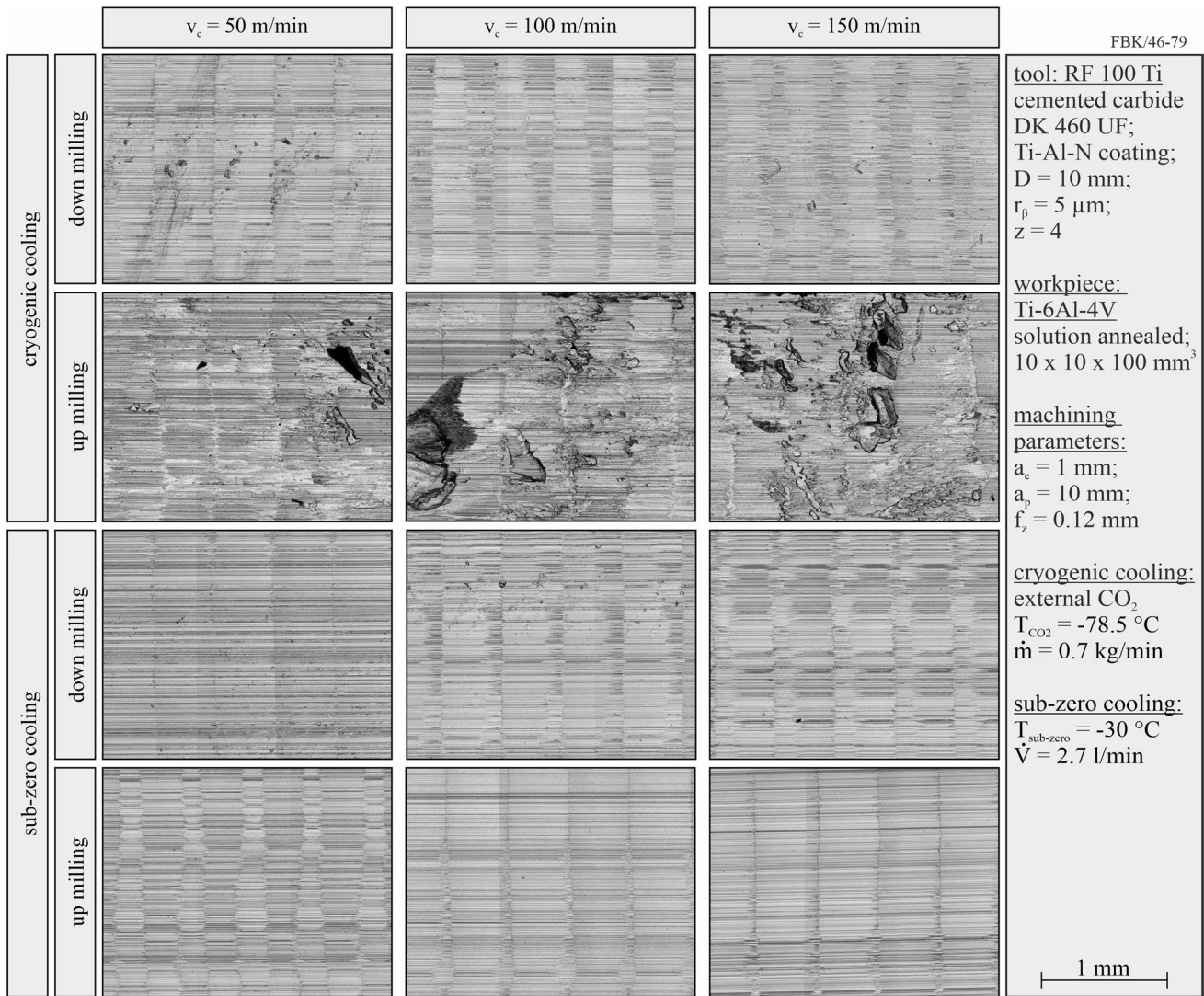


Fig. 11 Representative depiction of the surface topography at a constant feed per tooth of $f_z=0.12 \text{ mm}$ in dependence of the milling and cooling strategies

cooling offers beneficial lubrication effects which reduce friction within the cutting zone and promote the reduction of the thermal load. The lubrication effects and the high pressure that is used to supply the liquid sub-zero MWF are also beneficial to sufficiently remove chips from the cutting without damaging the workpiece surface which is why no scratches are observed after sub-zero milling.

To further characterize the surface quality, the root mean square height was measured to quantify the respective influence of the milling process and the cooling strategy. In Fig. 12, the surface roughness, quantified via the root mean square height, is depicted in dependence of the cutting parameters when down milling using a cryogenic and sub-zero cooling.

The influence of the cryogenic milling process during down milling is given in Fig. 12a. When increasing the feed

per tooth from $f_z=0.04$ to $f_z=0.08 \text{ mm}$, the root mean square height increases independent of the cutting speed due to an increase of the kinematic roughness. This is in line with the surface topographies depicted in Fig. 9 and Fig. 10. However, further increasing the feed per tooth to $f_z=0.12 \text{ mm}$ does not lead to higher root mean square heights measured (Fig. 12a), despite the increased kinematic roughness that is observed when comparing the images of the surface topography (see Fig. 10 and Fig. 11). While the kinematic roughness mainly refers to the roughness in feed direction, the root mean square height also takes the surface quality perpendicular to the feed direction into account. This could mean that the roughness perpendicular decreases when increasing the feed per tooth from $f_z=0.08$ to $f_z=0.12 \text{ mm}$, counteracting the higher kinematic roughness. Another possible explanation is given by smearing effects which could quench

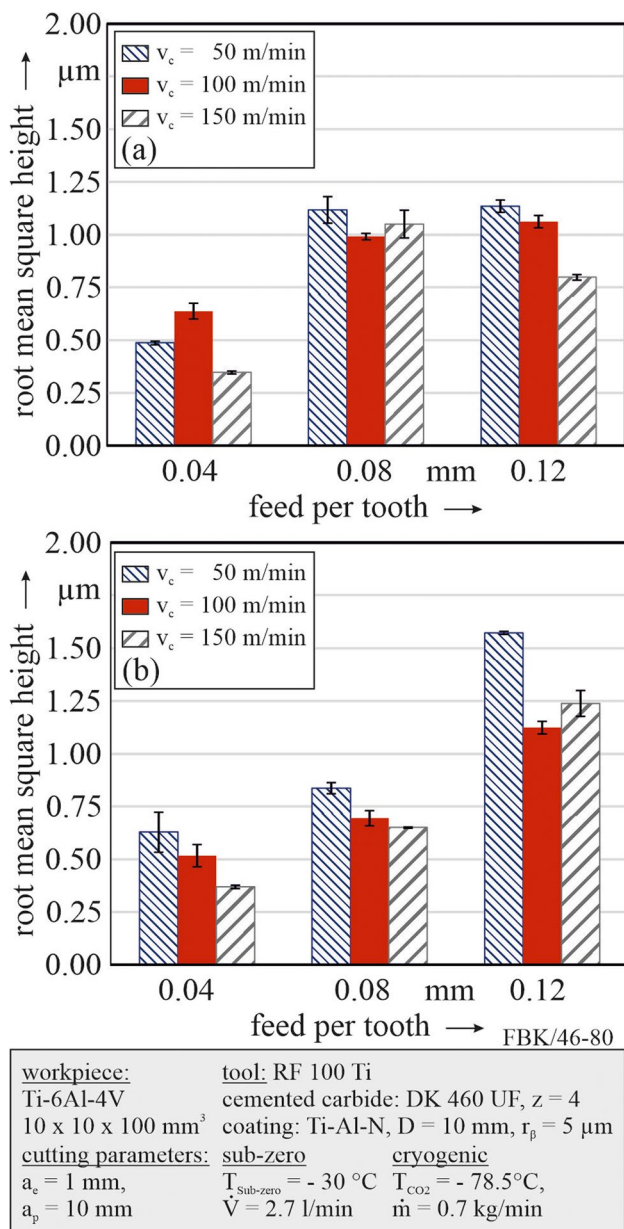


Fig. 12 Surface roughness in dependence of the cutting parameters when down milling using a cryogenic and b sub-zero cooling strategy

the workpiece material from the roughness peaks into the valleys resulting in lower root mean square heights. This quenching is promoted by higher mechanical and thermal loads due to ploughing and thermal softening. This becomes evident regarding the parameter combination of $f_z = 0.12 \text{ mm}$ and $v_c = 150 \text{ m/min}$ within Fig. 12a. Here a significant reduction of the root mean square height is observed since the elevated cutting speed promotes thermal softening while the high feed per tooth results in high mechanical loads.

For down milling (see Fig. 12b), an increase of the root mean square height is observed with increasing feed per

tooth, independent of the cutting speed. This consistent increase of the surface roughness at higher feeds per tooth is attributed to the kinematic roughness. With the exception of $f_z = 0.12 \text{ mm}$, the root mean square height decreased at higher cutting speeds when the feed per tooth is kept constant. This could also be explained by thermal softening enhanced by the increased cutting speed. Choosing the highest feed per tooth ($f_z = 0.12 \text{ mm}$) and the lowest cutting speed ($v_c = 50 \text{ m/min}$) results in the highest root mean square height measured for sub-zero down milling. This promotes the assumption that build-up edges could have occurred due to the unfavorable parameter combination, therefore decreasing the surface quality.

In Fig. 13a, the influence of the cryogenic milling process is depicted for up milling. When comparing to down milling (Fig. 12a), an increase of the root mean square height is observed for every parameter combination investigated. This can be explained by the promotion of ploughing effects during up milling. When increasing the feed per tooth and the cutting speed, the root mean square height and the respective standard deviation increase significantly. This is the result from the adhesions which are welded onto the workpiece surface for these respective cases (see. Figure 9, Fig. 10, and Fig. 11).

In Fig. 13b, the root mean square height is depicted for sub-zero up milling in dependence of the cutting parameters. At a constant cutting speed, an increase of the root mean square height is also observed at higher feeds per tooth for sub-zero up milling. In contrast to down milling, no significant influence of the cutting speed is observed at a constant feed per tooth of $f_z = 0.04 \text{ mm}$. At elevated feeds per tooth ($f_z \geq 0.08 \text{ mm}$), the root mean square heights even increase with higher cutting speeds. Therefore, it is assumed that the beneficial effects of the thermal softening are counteracted by the promoted ploughing effects during up milling. These ploughing effects are also enhanced at higher cutting speeds. Here, the increasing thermal load at higher cutting speeds leads to a higher ductility of the workpiece material which does promote ploughing.

When comparing the overall performance of the cooling strategies regarding the surface quality, the sub-zero cooling outperforms the cryogenic CO_2 cooling for the majority of the cases investigated. This becomes especially evident during up milling, as the sub-zero cooling successfully prevents adhesions on the workpiece surface due to a sufficient cooling capacity and beneficial lubrication effects. These lubrication effects also generally promote better surface qualities for down milling in comparison to the cryogenic cooling. However, when choosing the highest feed per tooth ($f_z = 0.12 \text{ mm}$) during down milling, cryogenic milling seemingly produces better surface qualities, since smaller root mean square heights are measured here. This is due to the promoted thermal softening, resulting in smearing effects

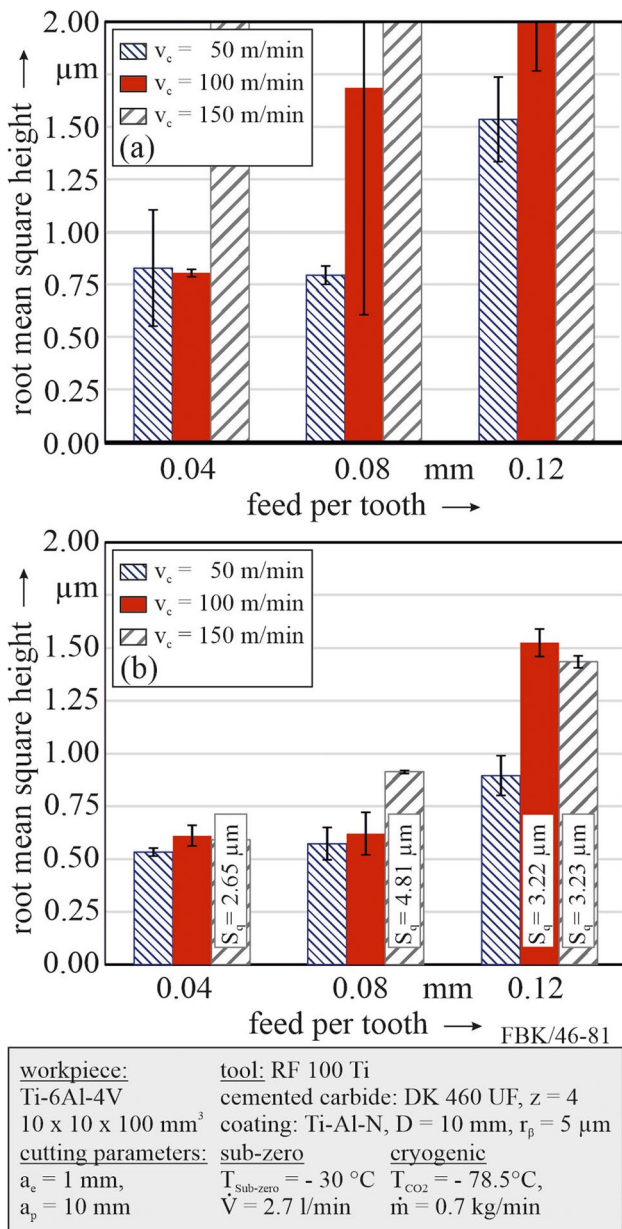


Fig. 13 Surface roughness in dependence of the cutting parameters when up milling using a cryogenic and b sub-zero cooling strategy

since higher thermal loads are expected here for cryogenic milling in comparison to sub-zero milling, that in general also stand for worse surface qualities (despite lower root mean square heights).

4 Summary

Within this investigation, the performance of a novel sub-zero cooling strategy was compared to cryogenic CO₂ cooling when milling Ti-6Al-4V. Besides the cooling strategy,

the cutting parameters as well as the milling strategy were systematically varied. The influence of the milling process and the two cooling strategies was characterized by analyzing the occurring forces, the resulting tool wear, and the resulting surface quality.

The highest impact on the occurring forces was observed when changing the feed per tooth, regardless of whether the cryogenic or sub-zero cooling was used. In contrast, the influence of the cutting speed on the occurring forces was comparably low for sub-zero milling. When using the cryogenic cooling, the increase of the cutting speed led to higher forces, particularly during up milling. This increase of the resulting forces was attributed to an increasing tool wear mainly characterized via adhesions at the cutting edge.

Adhesions at the cutting edge were mainly observed during up milling with the cryogenic CO₂ cooling. The amount of adhesions did increase significantly when increasing the feed per tooth and especially the cutting speed. This results from the very high thermal loads in the cutting zone that are promoted at high cutting speeds and due to friction caused by the ploughing effects during up milling. No significant tool wear was observed after sub-zero milling, regardless of the cutting parameters and the milling strategy. Despite unfavorable cutting conditions, the sub-zero cooling is able to sufficiently decrease the thermal load due to a high cooling capacity and favorable lubrication effects. As a consequence, no adhesions did occur.

When regarding the surface quality, the sub-zero cooling did outperform the cryogenic cooling as well for the majority of cases investigated. The usage of the sub-zero cooling led to less artifacts on the workpiece surface like scratches or adhesions even for unfavorable cutting conditions. For up milling, no suitable surface quality could be realized via cryogenic milling, due to a significant amount of adhesions. In contrast, a suitable surface quality was achieved when using the sub-zero cooling strategy.

It can therefore be concluded that the highly efficient cooling capacity of the sub-zero cooling strategy in superposition with the beneficial lubrication effects is capable to significantly reduce the thermal load when milling Ti-6Al-4V. Consequently, the sub-zero cooling outperforms the cryogenic cooling strategy regarding tool wear and surface quality, especially for up milling. As a result, the application of a sub-zero cooling strategy significantly improves the machinability of Ti-6Al-4V when milling, thus offering high potential to optimize the milling process regarding material removal rate and/or tool life.

In future investigations, the potential of the sub-zero cooling strategy for milling operation will be examined in more detail. In particular, the improvement of tool life for milling Ti-6Al-4V with a sub-zero MWF is of great interest. Moreover, the performance of this novel sub-zero cooling approach will be compared to other cooling strategies with industrial

relevance such as flood cooling and minimum quantity lubrication. Due to its superior cooling capacity, the application of sub-zero MWF could also be of high interest for various other processes like drilling or grinding, or other hard-to-cut materials like Inconel 718.

Author contribution All authors contributed to the study conception and design. Data collection and analysis were performed by Kevin Gutzeit, Georgis Bulun, and Gerhard Stelzer. The first draft was written by Kevin Gutzeit and all authors commented on previous versions of the manuscript. All authors read and approved the final manuscript.

Funding Open Access funding enabled and organized by Projekt DEAL. This work was funded by the Deutsche Forschungsgemeinschaft (DFG, German Research Foundation)—project number 172116086—SFB 926.

Declarations

Competing interests The authors declare no competing interests.

Disclaimer ¹Naming of specific manufacturers is done solely for the sake of completeness and does not necessarily imply an endorsement of the named companies nor that the products are necessarily the best for the purpose.

Open Access This article is licensed under a Creative Commons Attribution 4.0 International License, which permits use, sharing, adaptation, distribution and reproduction in any medium or format, as long as you give appropriate credit to the original author(s) and the source, provide a link to the Creative Commons licence, and indicate if changes were made. The images or other third party material in this article are included in the article's Creative Commons licence, unless indicated otherwise in a credit line to the material. If material is not included in the article's Creative Commons licence and your intended use is not permitted by statutory regulation or exceeds the permitted use, you will need to obtain permission directly from the copyright holder. To view a copy of this licence, visit <http://creativecommons.org/licenses/by/4.0/>.

References

1. Froes FHS, Gungor MN, Ashraf Imam M (2007) Cost-affordable titanium: the component fabrication perspective. *JOM* 59(6):28–31. <https://doi.org/10.1007/s11837-007-0074-8>
2. Williams JC, Boyer RR (2020) Opportunities and issues in the application of titanium alloys for aerospace components. *Metals* 10(6):705. <https://doi.org/10.3390/met10060705>
3. Gomez-Gallegos A, Mandal P, Gonzalez D, Zuelli N, Blackwell P (2018) Studies on titanium alloys for aerospace application. *DDF* 385:419–423. <https://doi.org/10.4028/www.scientific.net/DDF.385.419>
4. Inagaki I, Shirai Y, Takechi T, Ariyasu N (2014) Application and features of titanium for the aerospace industry. Nippon Steel Sumitomo Metal Technical Report 106:22–27
5. Schutz RW, Baxter CF, Boster PL, Fores FH (2001) Applying titanium alloys in drilling and offshore production systems. *JOM* 53(4):33–35. <https://doi.org/10.1007/s11837-001-0145-1>
6. Gurrappa I (2003) Characterization of titanium alloy Ti-6Al-4V for chemical, marine and industrial applications. *Mater Charact* 51(2–3):131–139. <https://doi.org/10.1016/j.matchar.2003.10.006>
7. Festas A, Ramos A, Davim JP (2022) Machining of titanium alloys for medical application - a review. *Proceedings of the Institution of Mechanical Engineers, Part B: Journal of Engineering Manufacture* 236(4):309–318. <https://doi.org/10.1177/09544054211028531>
8. Koizumi H, Takeuchi Y, Imai H, Kawai T, Yoneyama T (2019) Application of titanium and titanium alloys to fixed dental prostheses. *J Prosthodont Res* 63(3):266–270. <https://doi.org/10.1016/j.jpor.2019.04.011>
9. Ezugwu E, Bonney J, Yamane Y (2003) An overview of the machinability of aeroengine alloys. *J Mater Process Technol* 134(2):233–253. [https://doi.org/10.1016/S0924-0136\(02\)01042-7](https://doi.org/10.1016/S0924-0136(02)01042-7)
10. Barry J, Byrne G, Lennon D (2001) Observations on chip formation and acoustic emission in machining Ti-6Al-4V alloy. *Int J Mach Tools Manuf* 41(7):1055–1070. [https://doi.org/10.1016/S0890-6955\(00\)00096-1](https://doi.org/10.1016/S0890-6955(00)00096-1)
11. Ginting A, Nouari M (2009) Surface integrity of dry machined titanium alloys. *Int J Mach Tools Manuf* 49(3–4):325–332. <https://doi.org/10.1016/j.ijmactools.2008.10.011>
12. Pittalà GM, Monno M (2011) A new approach to the prediction of temperature of the workpiece of face milling operations of Ti-6Al-4V. *Appl Therm Eng* 31(2–3):173–180. <https://doi.org/10.1016/j.applthermaleng.2010.08.027>
13. Hua J, Shivpuri R (2005) A cobalt diffusion based model for predicting crater wear of carbide tools in machining titanium alloys. *J Eng Mater Technol* 127(1):136–144. <https://doi.org/10.1115/1.1839192>
14. Corduan N, Himbart T, Poulachon G, Dessoly M, Lambertin M, Vigneau J, Payoux B (2003) Wear mechanisms of new tool materials for Ti-6Al-4V high performance machining. *CIRP Ann* 52(1):73–76. [https://doi.org/10.1016/S0007-8506\(07\)60534-4](https://doi.org/10.1016/S0007-8506(07)60534-4)
15. Zoya Z, Krishnamurthy R (2000) The performance of CBN tools in the machining of titanium alloys. *J Mater Process Technol* 100(1–3):80–86. [https://doi.org/10.1016/S0924-0136\(99\)00464-1](https://doi.org/10.1016/S0924-0136(99)00464-1)
16. Cotterell M, Byrne G (2008) Dynamics of chip formation during orthogonal cutting of titanium alloy Ti-6Al-4V. *CIRP Ann* 57(1):93–96. <https://doi.org/10.1016/j.cirp.2008.03.007>
17. Rahman M, WANG ZG, WONG YS (2006) A review on high speed machining of titanium alloys. *JSMIE Int J Ser C* 49(1):11–20. <https://doi.org/10.1299/jsmec.49.11>
18. Dandekar CR, Shin YC, Barnes J (2010) Machinability improvement of titanium alloy (Ti-6Al-4V) via LAM and hybrid machining. *Int J Mach Tools Manuf* 50(2):174–182. <https://doi.org/10.1016/j.ijmactools.2009.10.013>
19. Aydın M, Köklü U (2022) Analysis of cutting forces at different spindle speeds with straight and helical-flute tools for conventional-speed milling incorporating the effect of tool runout. *Mech Based Des Struct Mach* 1–27. <https://doi.org/10.1080/15397734.2022.2125878>
20. Kaltenbrunner T, Krüchl HP, Schnalzger G, Klünsner T, Tepernegg T, Czettl C, Ecker W (2022) Differences in evolution of temperature, plastic deformation and wear in milling tools when up-milling and down-milling Ti6Al4V. *J Manuf Process* 77:75–86. <https://doi.org/10.1016/j.jmapro.2022.03.010>
21. Settineri L, Faga MG (2008) Nanostructured cutting tools coatings for machining titanium. *Mach Sci Technol* 12(2):158–169. <https://doi.org/10.1080/10910340802067239>
22. Wyen C-F, Wegener K (2010) Influence of cutting edge radius on cutting forces in machining titanium. *CIRP Ann* 59(1):93–96. <https://doi.org/10.1016/j.cirp.2010.03.056>
23. Zhuang K, Fu C, Weng J, Hu C (2021) Cutting edge microgeometries in metal cutting: a review. *Int J Adv Manuf Technol* 116(7–8):2045–2092. <https://doi.org/10.1007/s00170-021-07558-6>
24. Denkena B, Biermann D (2014) Cutting edge geometries. *CIRP Ann* 63(2):631–653. <https://doi.org/10.1016/j.cirp.2014.05.009>

25. Jawahir IS, Attia H, Biermann D, Dufflou J, Klocke F, Meyer D, Newman ST, Pusavec F, Putz M, Rech J, Schulze V, Umbrello D (2016) Cryogenic manufacturing processes. *CIRP Ann* 65(2):713–736. <https://doi.org/10.1016/j.cirp.2016.06.007>
26. Reitz W, Pendray J (2001) Cryoprocessing of materials: a review of current status. *Mater Manuf Processes* 16(6):829–840. <https://doi.org/10.1081/AMP-100108702>
27. Barber CR (1966) The sublimation temperature of carbon dioxide. *Br J Appl Phys* 17(3):391–397. <https://doi.org/10.1088/0508-3443/17/3/312>
28. Brinksmeier E, Meyer D, Huesmann-Cordes AG, Herrmann C (2015) Metalworking fluids—mechanisms and performance. *CIRP Ann* 64(2):605–628. <https://doi.org/10.1016/j.cirp.2015.05.003>
29. Pereira O, Rodríguez A, Fernández-Abia AI, Barreiro J, López de Lacalle LN (2016) Cryogenic and minimum quantity lubrication for an eco-efficiency turning of AISI 304. *J Clean Prod* 139:440–449. <https://doi.org/10.1016/j.jclepro.2016.08.030>
30. Ibrahim Sadik M, Isakson S, Malakizadi A, Nyborg L (2016) Influence of coolant flow rate on tool life and wear development in cryogenic and wet milling of Ti-6Al-4V. *Procedia CIRP* 46:91–94. <https://doi.org/10.1016/j.procir.2016.02.014>
31. Pittalà GM (2018) A study of the effect of CO2 cryogenic coolant in end milling of Ti-6Al-4V. *Procedia CIRP* 77:445–448. <https://doi.org/10.1016/j.procir.2018.08.278>
32. Iqbal A, Suhaimi H, Zhao W, Jamil M, Nauman MM, He N, Zaini J (2020) Sustainable milling of Ti-6Al-4V: investigating the effects of milling orientation, Cutter's helix angle, and type of cryogenic coolant. *Metals* 10(2):258. <https://doi.org/10.3390/met10020258>
33. Park K-H, Yang G-D, Suhaimi MA, Lee DY, Kim T-G, Kim D-W, Lee S-W (2015) The effect of cryogenic cooling and minimum quantity lubrication on end milling of titanium alloy Ti-6Al-4V. *J Mech Sci Technol* 29(12):5121–5126. <https://doi.org/10.1007/s12206-015-1110-1>
34. Wika KK, Gurdal O, Litwa P, Hitchens C (2019) Influence of supercritical CO2 cooling on tool wear and cutting forces in the milling of Ti-6Al-4V. *Procedia CIRP* 82:89–94. <https://doi.org/10.1016/j.procir.2019.04.169>
35. Tapoglou N, Lopez MIA, Cook I, Taylor CM (2017) Investigation of the influence of CO 2 cryogenic coolant application on tool wear. *Procedia CIRP* 63:745–749. <https://doi.org/10.1016/j.procir.2017.03.351>
36. Moon JH, Cho M, Lee SH (2016) Dynamic wetting and heat transfer characteristics of a liquid droplet impinging on heated textured surfaces. *Int J Heat Mass Transf* 97:308–317. <https://doi.org/10.1016/j.ijheatmasstransfer.2016.02.041>
37. Kirsch B, Basten S, Hasse H, Aurich JC (2018) Sub-zero cooling: a novel strategy for high performance cutting. *CIRP Ann* 67(1):95–98. <https://doi.org/10.1016/j.cirp.2018.04.060>
38. Basten S, Kirsch B, Hasse H, Aurich JC (2020) Formulation of sub-zero metalworking fluids for cutting processes: influence of additives. *CIRP J Manuf Sci Technol* 31:25–33. <https://doi.org/10.1016/j.cirpj.2020.09.006>
39. Basten S, Kirsch B, Merz R, Kopnarski M, Hasse H, C. Aurich J, (2020) Adsorption and reaction layers when turning AISI 304 using various cooling strategies. *Procedia CIRP* 87:125–130. <https://doi.org/10.1016/j.procir.2020.02.100>
40. Basten S, Kirsch B, Hasse H, Aurich JC (2021) Sub-zero metalworking fluids for high performance cutting of difficult to cut materials. *Procedia CIRP* 101:342–345. <https://doi.org/10.1016/j.procir.2020.11.016>
41. Ankener W, Uebel J, Basten S, Smaga M, Kirsch B, Seewig J, Aurich JC, Beck T (2020) Influence of different cooling strategies during hard turning of AISI 52100 – part II: characterization of the surface and near surface microstructure morphology. *Procedia CIRP* 87:119–124. <https://doi.org/10.1016/j.procir.2020.02.094>
42. Basten S, Kirsch B, Ankener W, Smaga M, Beck T, Uebel J, Seewig J, Aurich JC (2020) Influence of different cooling strategies during hard turning of AISI 52100 - part I: thermo-mechanical load, tool wear, surface topography and manufacturing accuracy. *Procedia CIRP* 87:77–82. <https://doi.org/10.1016/j.procir.2020.02.085>
43. Gutzeit K, Bulun G, Stelzer G, Kirsch B, Seewig J, Aurich JC (2022) Investigation of the surface integrity when cryogenic milling of Ti-6Al-4V using a sub-zero metalworking fluid. *Procedia CIRP* 108:25–30. <https://doi.org/10.1016/j.procir.2022.03.010>
44. Aydın M, Köklü U (2020) Analysis of flat-end milling forces considering chip formation process in high-speed cutting of Ti6Al4V titanium alloy. *Simul Model Pract Theory* 100:102039. <https://doi.org/10.1016/j.simpat.2019.102039>
45. Gutzeit K, Berndt M, Schulz J, Müller D, Kirsch B, Harbou E von, Aurich JC (2022) Optimization of the cooling strategy during cryogenic milling of Ti-6Al-4 V when applying a sub-zero metalworking fluid. *Prod Eng Res Devel*. <https://doi.org/10.1007/s11740-022-01178-z>
46. DIN EN ISO 25178–73:2019–10, Geometrische Produktspezifikation_(GPS)_- Oberflächenbeschaffenheit Flächenhaft_- Teil_73 Begriffe für Oberflächenfehler an Maßverkörperungen (ISO_25178–73:2019) Deutsche Fassung EN_ISO_25178–73:2019 Beuth Verlag GmbH Berlin <https://doi.org/10.31030/3041489>
47. Caudill J, Schoop J, Jawahir IS (2019) Numerical modeling of cutting forces and temperature distribution in high speed cryogenic and flood-cooled milling of Ti-6Al-4V. *Procedia CIRP* 82:83–88. <https://doi.org/10.1016/j.procir.2019.04.055>
48. Sutter G, List G (2013) Very high speed cutting of Ti–6Al–4V titanium alloy – change in morphology and mechanism of chip formation. *Int J Mach Tools Manuf* 66:37–43. <https://doi.org/10.1016/j.ijmactools.2012.11.004>
49. Hou J, Zhou W, Duan H, Yang G, Xu H, Zhao N (2014) Influence of cutting speed on cutting force, flank temperature, and tool wear in end milling of Ti-6Al-4V alloy. *Int J Adv Manuf Technol* 70(9–12):1835–1845. <https://doi.org/10.1007/s00170-013-5433-8>
50. Zain AM, Haron H, Sharif S (2010) Simulated annealing to estimate the optimal cutting conditions for minimizing surface roughness in end milling Ti-6Al-4V. *Mach Sci Technol* 14(1):43–62. <https://doi.org/10.1080/10910340903586558>
51. Karkalos NE, Galanis NI, Markopoulos AP (2016) Surface roughness prediction for the milling of Ti–6Al–4V ELI alloy with the use of statistical and soft computing techniques. *Measurement* 90:25–35. <https://doi.org/10.1016/j.measurement.2016.04.039>

Publisher's Note Springer Nature remains neutral with regard to jurisdictional claims in published maps and institutional affiliations.